Full Length Article

The microbial metagenome and bone tissue composition in mice with microbiome-induced reductions in bone strength

Jason D. Guss[a,b], Erik Taylor[a], Zach Rouse[c], Sebastian Roubert[a], Catherine H. Higgins[d],
Corinne J. Thomas[e], Shefford P. Baker[c], Deepak Vashishth[e], Eve Donnelly[c,f], M. Kyla Shea[g],
Sarah L. Booth[g], Rodrigo C. Bicalho[d], Christopher J. Hernandez[a,b,f,*]

[a] Sibley School of Mechanical and Aerospace Engineering, Cornell University, Ithaca, NY, USA
[b] Meinig School of Biomedical Engineering, Cornell University, Ithaca, NY, USA
[c] Material Science and Engineering, Cornell University, New York, NY, USA
[d] College of Veterinary Medicine, Cornell University, Ithaca, NY, USA
[e] Department of Biomedical Engineering, Center for Biotechnology and Interdisciplinary Studies, Rensselaer Polytechnic Institute, Troy, NY, USA
[f] Hospital for Special Surgery, New York, NY, USA
[g] Jean Mayer USDA Human Nutrition Research Center on Aging, Tufts University, Boston, MA, USA

ARTICLE INFO

ABSTRACT

The genetic components of microbial species that inhabit the body are known collectively as the microbiome. Modifications to the microbiome have been implicated in disease processes throughout the body and have recently been shown to influence bone. Prior work has associated changes in the microbial taxonomy (phyla, class, species, etc.) in the gut with bone phenotypes but has provided limited information regarding mechanisms. With the goal of achieving a more mechanistic understanding of the effects of the microbiome on bone, we perform a metagenomic analysis of the gut microbiome that provides information on the functional capacity of the microbes (all microbial genes present) rather than only characterizing the microbial taxa. Male C57Bl/6 mice were subjected to disruption of the gut microbiota (ΔMicrobiome) using oral antibiotics (from 4 to 16 weeks of age) or remained untreated (n = 6–7/group). Disruption of the gut microbiome in this manner has been shown to lead to reductions in tissue mechanical properties and whole bone strength in adulthood with only minor changes in bone geometry and density. ΔMicrobiome led to modifications in the abundance of microbial genes responsible for the synthesis of the bacterial cell wall and capsule; bacterially synthesized carbohydrates; and bacterially synthesized vitamins (B and K) (p < 0.01). Follow up analysis focused on vitamin K, a factor that has previously been associated with bone health. The vitamin K content of the cecum, liver and kidneys was primarily microbe-derived forms of vitamin K (menaquinones) and was decreased by 32–66% in ΔMicrobiome mice compared to untreated animals (p < 0.01). Bone mineral crystallinity determined using Raman spectroscopy was decreased in ΔMicrobiome mice (p = 0.01). This study illustrates the use of metagenomic analysis to link the microbiome to bone phenotypes and provides preliminary findings implicating microbially synthesized vitamin-K as a regulator of bone matrix quality.

1. Introduction

The gut microbiome consists of the genomic components, products, and microorganisms in the gastrointestinal tract [1]. Changes in the constituents of the microbiome have been associated with a number of chronic diseases throughout the body including cardiovascular disease, obesity, diabetes, Alzheimer's disease and arthritis [1]. The effects of the microbiome on host physiology have resulted in considerable interest in the microbiome as a potential diagnostic or therapeutic target [2].

Recent studies have indicated that the microbiome can have a profound effect on bone: mice raised from birth in an environment completely absent of microbial life (germ-free) have altered long bone length and trabecular and cortical bone mass [3–5]. Disruption of the gut microbiome using oral antibiotics lead to changes in trabecular and cortical bone mass and femoral geometry in mice [5–9]. Manipulation of the gut microbiome with probiotics has been shown to reduce bone loss associated with estrogen depletion in mice [10–12] and recent

---

studies have suggested a similar effect in humans [13]. Together these findings implicate the microbiome as a contributor to bone mass and bone mineral density and thereby influence fracture risk. However, bone mineral density does not completely explain fracture risk [14,15]. The term "bone quality" is used to refer to characteristics of bone other than bone mineral density that influence bone strength and fracture risk [16]. We recently demonstrated that disruption of the gut microbiome in mice led to reductions in femoral whole bone strength that could not be explained by changes in bone mass and geometry, indicating that modifications to the microbiome lead to impaired bone tissue quality (Fig. 1A) [8].

To date, studies reporting an effect of the microbiome on bone have characterized the microbiome using sequencing of the bacterial 16S rRNA gene to determine the relative abundance of microbial taxa (phylum, class, order, etc.) [3,5,8,17]. While phylogeny is useful for understanding the microbial community, more detailed sequencing is required to identify molecular pathways that link the microbiome to host phenotype. Metagenomic sequencing involves analysis of the entire microbial genome and provides information on the functional capacity of the gut microbiome (i.e. which genes are present) [18,19]. Metagenomic analysis is useful because many interactions between the microbiota and the host are a result of microbial functional capacity rather than microbial taxonomy.

Changes in the composition and structure of the organic or mineral composition of bone can lead to changes in both tissue- and whole bone mechanical performance [20–22]. Bone tissue chemical composition can be assessed using Raman spectroscopy to determine: crystallinity (the size and stoichiometric perfection of the hydroxyapatite crystal lattice), mineral-to-matrix ratio (the extent of collagen mineralization and mineral content), and the carbonate-to-phosphate ratio (the extent of carbonate substitution into hydroxyapatite crystals). Additionally, nanoindentation can characterize compressive mechanical properties (hardness and reduced modulus) at the tissue-scale [20]. To our knowledge, metagenomic analysis of the microbiome has not yet been used to understand the effects of the microbiome on bone. Additionally, although multiple studies report modifications in bone composition and nanomechanical properties in the context of bone quality and fracture risk [21,23–26], no previous studies have evaluated changes in bone tissue composition associated with changes in the gut microbiome.

The goal of this line of investigation is to determine how modifications to the gut microbiome can influence bone tissue quality. Using samples from a previously reported study including microbiome-induced changes in bone strength (Fig. 1A), we performed metagenomic analysis of the fecal microbiota as well as nanoscale chemical analysis of bone tissue. Specifically, we determined the changes in the fecal metagenome and bone tissue chemical composition and nanomechanical properties associated with microbiome-induced changes in bone tissue strength.

2. Material and methods

2.1. Study design

Animal procedures were approved by Cornell University's Institutional Animal Care and Use Committee. Mice from the C57BL/6 J inbred strain were acquired (Jackson Laboratory, Bar Harbor, ME) and bred in conventional housing in our animal facility. Male mice were either treated to modify the gut microbiome (ΔMicrobiome) or untreated. Treated animals received broad-spectrum antibiotics (1.0 g/L ampicillin + 0.5 g/L neomycin) in their drinking water from weaning at 4 weeks of age until skeletal maturity (16 weeks of age) [27]. Chronic antibiotics cause disruptions to the gut microbiome that are maintained over a prolonged time period [28]. The oral bioavailability of these antibiotics is absent (neomycin) or low (ampicillin), thereby limiting extra-intestinal effects of dosing [27,29]. Additionally, neomycin and ampicillin have never been associated with impaired bone growth, do

not cause considerable changes bone length, body mass or gut inflammation in these animals [8] and do not cause noticeable changes in serum calcium or vitamin D. Neomycin primarily targets Gram negative organisms while ampicillin is more broad spectrum. Animals were housed in plastic cages filled with 1/4-inch corn cob bedding (The Andersons' Lab Bedding, Maumee, Ohio), fed with standard laboratory chow (Teklad LM-485 Mouse/Rat Sterilizable Diet) and water ad libitum, and provided a cardboard refuge environmental enrichment hut (Ketchum Manufacturing, Brockville, Ontario). Animals were euthanized at 16 weeks of age. The right tibia, right humerus, cecum, liver, kidney, and fecal samples were collected. Bone, kidney and liver were stored at −20 °C and cecum and fecal samples were stored at −80 °C.

The study was performed using two cohorts of animals. One cohort of animals, described in a prior study [8], was used for metagenomic analysis and tissue chemical, nanomechanics and biochemistry (ΔMicrobiome n = 7, untreated n = 8). Tissue for some of the follow up biochemical analyses used samples from a second cohort of animals raised in our facility under identical conditions (untreated: n = 6).

2.2. Metagenomic analysis

Fecal samples collected one day prior to euthanasia were used for metagenomics analysis. Metagenomic analysis was performed on six samples per group (2 animals per cage). DNA was extracted (DNeasy PowerSoil DNA Isolation Kit, MO BIO Laboratories Inc., Carlsbad, CA) following manufacturer's recommendations. The fecal pellet was added to the PowerBead tubes (Qiagen, Germantown, MD) and followed by a 10-minute vortex step. Following addition of Solution C1, to enhance cell lysis, samples were incubated at 70 °C for 10 min and then subjected to a vortex step for 15 min using the MO BIO Vortex Adapter tube holder. Isolated DNA was quantified (Qubit dsDNA Broad Range Assay Kit, Life Technologies, Carlsbad, CA). Aliquots of DNA were normalized to the same concentration of 0.2 ng/ul of DNA per sample. A sequence library was prepared (Nextera XT DNA Library Preparation Kit, Illumina, San Diego, CA) to yield an average library size of 500 bp. Final equimolar libraries were sequenced (MiSeq reagent kit v3 on the MiSeq platform, Illumina, San Diego, CA) to generate 300 bp paired-end reads [30].

Metagenomic analyses were performed using MG-RAST (Metagenome Rapid Annotation using Subsystem Technology version 4.0.3) [31,32]. In the MG-RAST analysis, the fragments of DNA in a sample are compared to protein, RNA, and subsystem databases. Functional annotation of sequences in the current study used the SEED subsystem [33]. The functional abundance analysis was performed using a "Representative Hit Classification" approach with a maximum e-value of 1×10^{-5}, minimum identity of 60%, and a minimum alignment length of 15 measured in amino acids for proteins and base pairs for RNA databases. The subsystems are grouped into hierarchical classifications ranging from the broadest functional category at "Level 1", to more specific functional roles at "Level 2" and "Level 3", and then to the most detailed category of "Function". The data underwent a normalization and standardization process (within MG-RAST) to reduce inter-sample variability and to allow data to be more easily comparable. The normalized counts were calculated as: $normalized_i = log\,2(raw_{counts_i} + 1)$. The standardized counts were calculated as: $standardized_i = (normalized_i - mean(normalized_i))/stdev(normalized_i)$. Normalized counts are used as a measure of the abundance of genes that match a functional category. Differences in the abundance of genes in each of the functions were identified with $\alpha = 0.05$ [34,35].

Principal coordinate analysis (PCoA) of the functional hierarchy based on the Bray-Curtis distance was performed to investigate overall functional diversity of the microbiota. Principal coordinate analysis reduces the dimensionality of a complex dataset with thousands of variables to a smaller number so the diversity between samples can be easily visualized in a two- or three-dimensional scatterplot [36]. Each

principal coordinate explains a percentage of the variation in the data set, with the first two principal components accounting for the most variation. PCoA was performed at subsystem Level 1, Level 2, and Level 3 hierarchies. Differences between groups at Level 1 was determined using Analysis of Similarity (ANOSIM, implemented using the vegan package for R, v.2.4-2, https://www.rdocumentation.org/packages/vegan).

2.3. Biochemical analysis

Biochemical analyses of tissues were performed after receiving the results of the metagenomics analysis as a means of testing the functional significance of modifications to the microbial metagenome (n = 6/group). Based on the metagenomics findings and bone biomechanical findings, the biochemical analysis focused on vitamin K. Vitamin K is a class of fat-soluble vitamers consisting of phylloquinone (PK, vitamin K_1 in older literature) and the menaquinones (vitamin K_2 in older literature). Menaquinones exist in ten known forms, identified by the length of the isoprenoid side chain of the molecule (labeled MK-n where n is the length of the side chain, MK4-MK13) [37]. Phylloquinone and MK-4 are derived primarily from the diet. The remaining nine known forms of menaquinone are synthesized primarily by bacteria in the gut, although some bacterially-derived forms of vitamin K are found in fermented or cured food products [37]. The cecum is an important site for microbial production of vitamin K [38] and the liver and kidney are distant organs where vitamin K accumulates [39], hence phylloquinone (PK) and menaquinone (MK-4-13) concentrations in the cecum, liver and kidney were measured by liquid chromatography/mass spectroscopy (LC/MS) [40]. Detailed procedures for vitamin K extraction and sample purification are described elsewhere [40]. The LC/MS system consists of an Agilent 6130 Quadrupole MSD with an atmospheric pressure chemical ionization (APCI) source connected to an Agilent series 1260 HPLC instrument (Agilent Technologies, Santa Clara, CA). Separations were completed using a reversed-phase C18 analytical column (Kinetex 2.6 μm, 150 mm × 3.0 mm; Phenomenex, Inc., Torrance, CA).

A major function of vitamin K in bone is carboxylation of Gla-containing proteins during bone formation. The most abundant Gla-containing protein in bone matrix is osteocalcin (also the most abundant non-collagenous protein in bone). Protein extraction was performed using a protein extraction technique with improved yield from bone without requiring demineralization [41]. The humeri were homogenized to a fine past in 600 μL of extraction buffer containing 0.05 M EDTA, 4 M guanidine chloride and 30 mM Tris-HCl (Omni BeadRuptor 24, Omni International, Atlanta, GA). After homogenization, the solution was centrifuged at 13000 rpm for 15 min to eliminate remaining mineral debris from the supernatant. The supernatant was dialyzed against 1× PBS and 5 mM EDTA for two days to eliminate denaturant. Extracted bone protein concentrations of the dialyzed solutions were assessed using a Pierce Coomassie Plus (Bradford) Assay Kit (Thermo-Fisher Scientific, Waltham, MA, USA). The extracts then were serially diluted 1000-fold in PBS for use with the Mouse Osteocalcin ELISA kit (LSBio, Seattle, WA, USA), which has a working range of 0.156–10 ng/mL. The OC quantification ELISA was performed as per manufacturer protocol. Osteocalcin content was assessed in triplicate in 4–5 animals per group and the average value was determined (intra-assay coefficient of variation = 0.07 ± 0.05).

2.4. Bone tissue characterization

The right tibiae were harvested and fixed in 10% neutral buffered formalin as part of a separate analysis. Tibiae were then dehydrated in ethanol and embedded undecalcified in methyl methacrylate and a single 2-mm-thick transverse section from the proximal metaphysis was collected using a diamond wafering saw (Buehler, Lake Bluff, Illinois). All sections were polished anhydrously on a Multiprep automatic

polishing system (Allied High Tech, Rancho Dominguez, CA) at 30 RPM with a 200 g sample load. Samples were polished with increasing grit silicon carbide polishing paper (800, 1200 grit) using ethylene glycol as a lubricant, and followed by a series of slurries of aluminum oxide powder (particle size of 3 μm, 1 μm, and 0.1 μm) in ethylene glycol [42]. The final root mean square (RMS) roughness of the surface was determined to be ~35 nm by measurement of ten 5×5-μm^2 scans per sample with a surface profilometer (VKX Laser-Scanning Microscope; Keyence, Inc.).

A Raman imaging system (InVia Confocal Raman Microscope; Reinshaw Inc.) was used to collect spectra of the tibial cross sections by analyzing four different regions in each cross section (n = 4/group). A total of 20 individual point spectra were collected across four quadrants of the cross section. Five point spectra were collected in each quadrant forming a '+' sign centered mid-thickness (points were at least 50 μm from each other). These points were selected to avoid recently formed bone tissue which can have different material properties from tissue that has completed primary mineralization. The five spectra were averaged to determine a single representative measure per quadrant per sample. Spectra were collected over the range 720–1820 cm^{-1} with a 785 nm laser and a 50× long-working-distance objective (N.A. = 0.55) collecting for 30s at 50% power with cosmic ray correction. Spectra first were normalized to the absorbance of PMMA at 813 cm^{-1} (MATLAB, MathWorks). Last, spectra were baseline-corrected to account for background fluorescence. The following Raman bands were evaluated: phosphate (PO_4^{3-}) $\nu_1 PO_4$ (integration area ~930–980 cm^{-1}) [43] and amide III (integration area ~1215–1300 cm^{-1}) [43]. From each spectrum mineral-to-matrix ratio (determined as the area ratio of phosphate $\nu_1 PO_4$ and amide III) and mineral crystallinity (the inverse of the full-width-half-max of a Gaussian fit of the phosphate $\nu_1 PO_4$ peak) were measured [44]. Raman spectroscopy was limited to these two measures as they are not sensitive to the tissue fixation protocol [45]. During Raman spectroscopy, native tissue specimens were oriented with the longitudinal axis of bone horizontal on the stage to minimize effects of variations in microstructural orientation with respect to the incident beam on the measured intensity.

Nanoindentation was performed on the same sections and regions analyzed by Raman spectroscopy. Nanoindentation arrays were performed using a Berkovich indenter tip (TI-900 Triboindenter, Bruker, Eden Prairie, MN) calibrated to a silica glass standard. Each array consisted of a 4×4 grid of indentations with a 30 s ramp load to $P_{max} = 2500$ μN, a 30 s hold to reach equilibrium, and a five-second elastic unloading. Indents were placed 15 μm away from each other to avoid mechanical interactions among indentations. The nominal contact depth of the indents in the bone samples was 260 nm. Hardness (H) and reduced modulus (E_r) were determined from the force vs. displacement curves of each indentation [46] using the following relations:

$$H = \frac{P_{max}}{A_c}, \qquad E_r = \frac{S\sqrt{\pi}}{2\sqrt{A_c}},$$

for which S is the contact stiffness (the slope of the load-displacement curve upon initial unloading) and A_c is the projected contact area of the indentation. Hardness and reduced modulus characterize the ability of the material to resist indentation, a trait that is sometimes correlated with tissue strength.

2.5. Statistical treatment

Group differences between nanoindentation measures, metagenome sequence abundances, vitamin K levels, and osteocalcin content were determined using a one-way ANOVA α = 0.05 (JMP Pro 9.0.0). Differences in Raman measures between groups were determined using a generalized least squares model (GLM) to account for the effect of
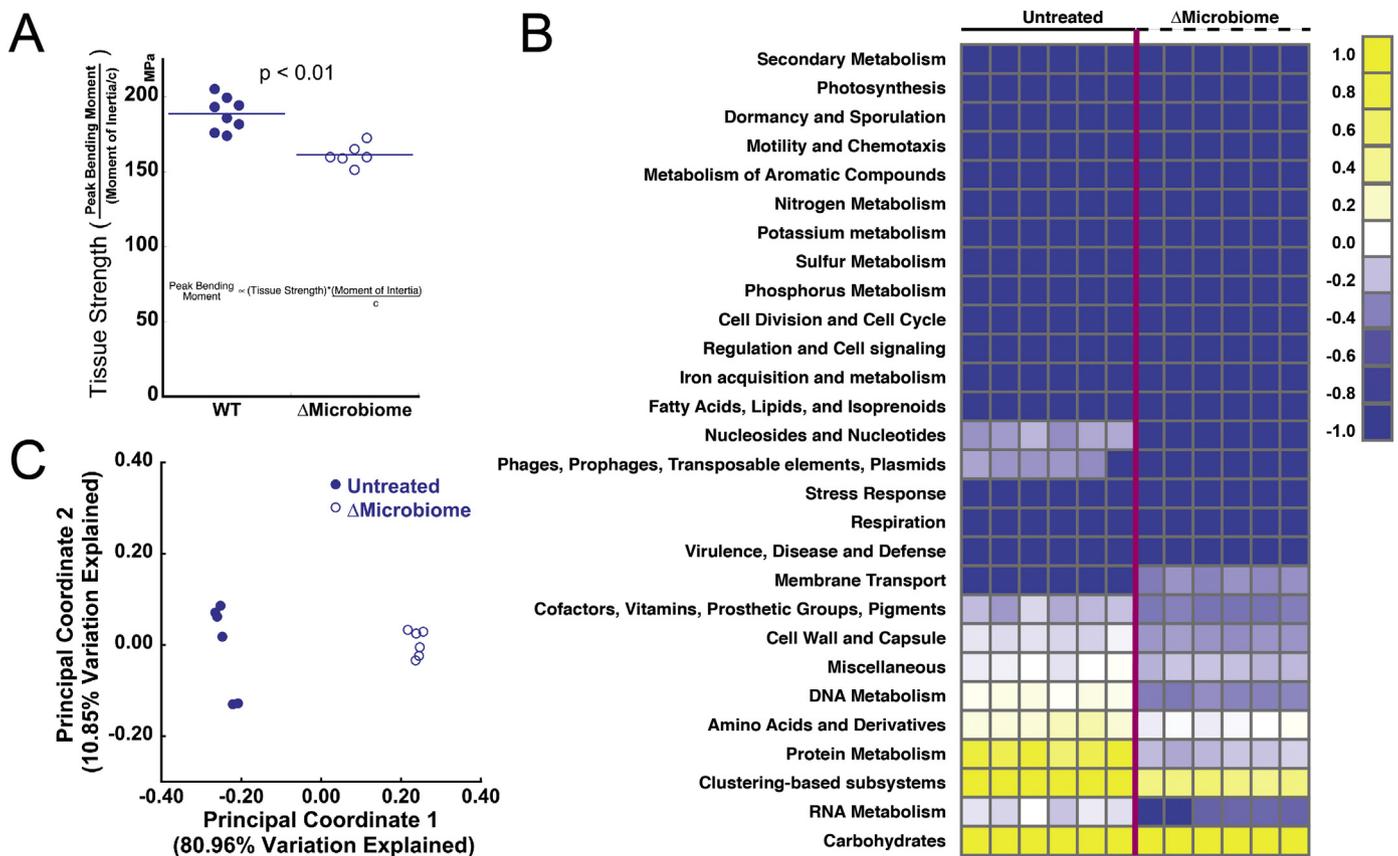
Fig. 1. (A) Disruption of the gut microbiome (ΔMicrobiome) results in reductions in tissue strength assessed through three point bending of the mouse femur (figure adapted from [8]). (B) A heatmap summarizing the metagenomic analysis of the fecal microbiota. Each column represents an individual animal (n = 6 per group). (C) Principal coordinate analysis summarizes the differences in the functional capacity of the gut microbiota between the two groups (p = 0.003, R^2 = 0.93, ANOSIM).

quadrant.

3. Results

3.1. Metagenome functional analysis

The functional capacities of the gut microbiome differed among groups (Fig. 1B). Disruption of the gut microbiome caused drastic changes in the functional capacity of the gut microbiome, as indicated by distinct clusters in the principal coordinate analysis (Fig. 1C). Metagenomics findings indicated differences in the abundance of genes associated with vitamin biosynthesis, carbohydrate function and cell and cell capsule synthesis.

Pathways related to the synthesis of vitamin B and vitamin K were altered by disruption of the gut microbiome. Mice with a disrupted gut microbiome had lower normalized counts for genes associated with the synthesis of vitamin B2, B6, and B7 compared to untreated mice (Fig. 2A), but had greater normalized counts for genes involved in the synthesis of vitamin B9 and K. Further investigation identified differential presence of multiple genes involved in menaquinone biosynthesis (Fig. 2B): normalized counts for MenB, MenC and MenG genes were less in ΔMicrobiome mice than in untreated mice while counts for MenH, MenF, and MenE genes were greater in ΔMicrobiome mice.

The overall functional capacity and the abundance of genes for six of eight carbohydrate functional categories were altered by ΔMicrobiome (Fig. 2C, Supplemental Fig. 1, no differences in amino-sugars and fermentation were detected). No differences in the overall abundance of fermentation genes were detected. The abundance of genes related to the cell wall and cell capsule differed among groups (Fig. 2D). Normalized counts for genes for capsular and extracellular polysaccharides were less abundant in mice with a disrupted gut microbiome than in untreated mice (p < 0.002). Disruption of the gut microbiome led to increased abundance of genes associated with Gram-negative cell wall components.

3.2. Biochemical analysis

Vitamin K content in the cecum, liver, and kidney primarily consisted of microbe-derived menaquinones; on average, the microbe-derived menaquinones (MK5-13) accounted for 83.3% to 99.9% of the total vitamin K content (Fig. 3A–C, Supplementary Table 1). Total cecal vitamin K content was lower in ΔMicrobiome mice compared to untreated mice (Fig. 3A). In the cecum, disruption of the gut microbiome led to drastic changes in the forms of vitamin K that were present (reduced MK10 and MK11 and increased MK7 and MK8). Total liver vitamin K content was lower in ΔMicrobiome compared to untreated mice (Fig. 3B). In the liver, disruption of the gut microbiome led to reduced concentration of MK11 and increases in MK4 and MK6. Kidney vitamin K content was also decreased in ΔMicrobiome mice, although there were no noticeable changes in the forms of menaquinone present (Fig. 3C). Mean matrix-bound osteocalcin concentration showed a trend indicated reduced concentration in ΔMicrobiome mice (p = 0.05, Fig. 3D).

3.3. Raman spectroscopy and nanoindentation

Bone tissue crystallinity and mineral to matrix ratio varied among quadrants (p < 0.05, Fig. 4). After accounting for variation among quandrants, disruption of the gut microbiome was associated with decreased crystallinity (p = 0.01, average difference 1.1%) and no
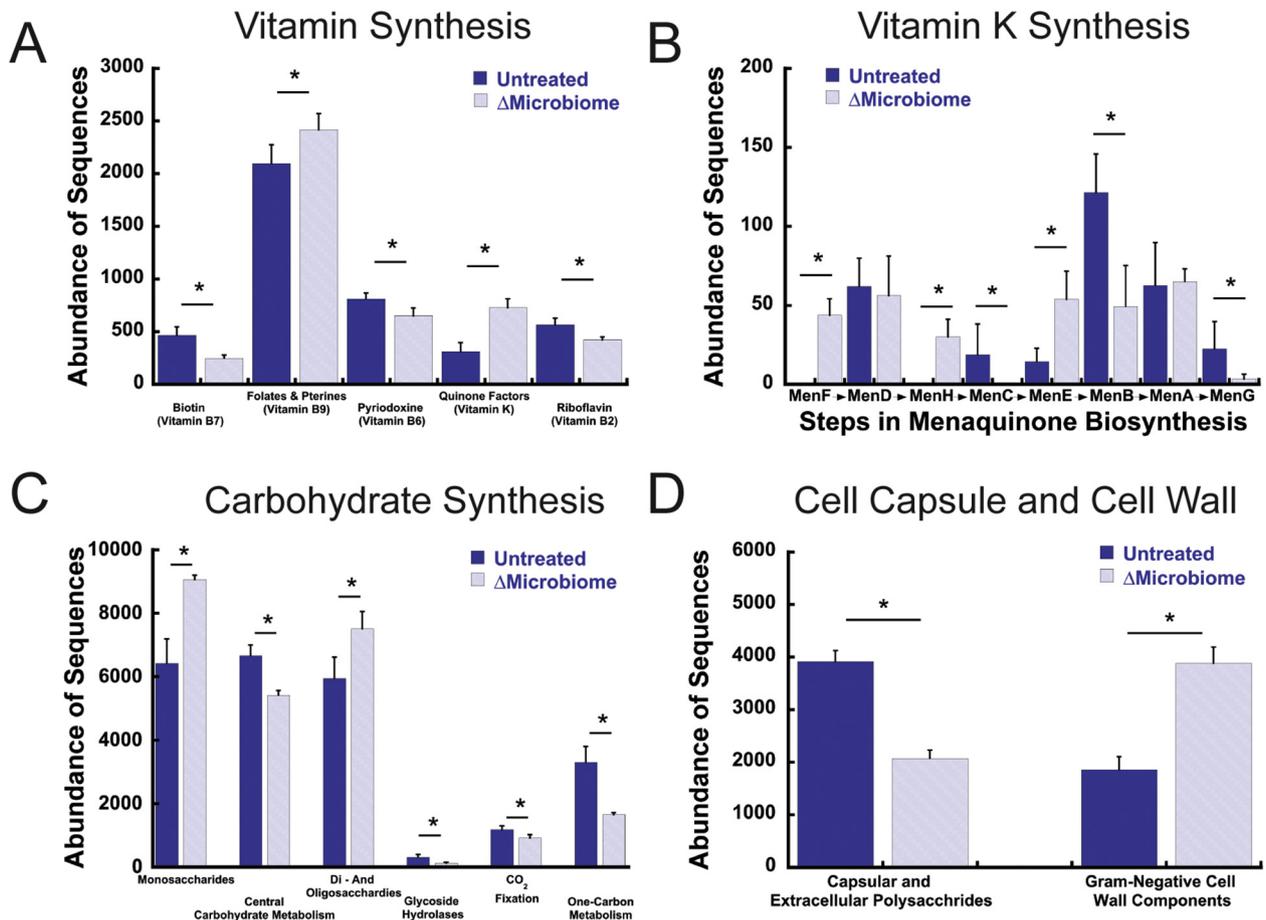
Fig. 2. The relative abundance of genes associated with key pathways for (A) vitamin synthesis, (B) vitamin K synthesis (shown in the order of synthesis), (C) carbohydrates, and (D) bacterial cell wall and capsule components are altered in ΔMicrobiome mice (n = 6/group). * - p < 0.002. Effect size is shown in Supplementary Fig. 1.

detectable differences in mineral:matrix (Fig. 4B–C). Subsequent high density mapping in the posterior region of the bone revealed a similar trends in crystallinity (p = 0.09, Supplemental Fig. 2) and mineral:matrix ratio.

Reduced modulus measured using nanoindentation was similar among groups (Supplemental Fig. 3; untreated: 30.8 GPa ± 1.06; ΔMicrobiome: 30.4 GPa ± 1.20, mean ± SD). Hardness was similar among groups (Supplemental Fig. 3; untreated: 1.08 GPa ± 0.07; ΔMicrobiome: 1.09 GPa ± 0.04).

4. Discussion

This study provides the first report of the differences in the metagenomic components of the microbiome associated with altered bone. The metagenomic analysis identified differences among groups in terms of the abundance of genes related to vitamin synthesis, cell wall and capsule synthesis, and carbohydrate synthesis. The observed differences in the abundance of genes associated with vitamin synthesis led to follow up biochemical analyses focused on vitamin K, a factor that has long been associated with bone health [47,48]. Biochemical analysis confirmed reduced concentrations of vitamin K in the cecum, liver and kidney associated with disruption of the gut microbiota – an effect dominated by reductions in the concentrations of forms of vitamin K generated by microbes (menaquinones 5–13), supporting a potential link between vitamin K produced by the gut microbiota and bone tissue quality.

The current study provides a metagenomic analysis as a means to identify potential mechanistic relationships between disruption of the gut microbiome and impaired bone tissue strength (Fig. 1A). The gut microbiome may influence bone tissue through three general mechanisms: 1) regulation of nutrient absorption and microbe-derived vitamins; 2) regulation of the immune system; and 3) translocation of inflammatory bacterial products across the gut barrier [49]. While regulation of the immune system and translocation of inflammatory bacterial products can lead to changes in bone resorption, bone formation and bone mass [50], these mechanisms do not directly regulate bone matrix quality; modification to bone resorption/formation alone primarily influence bone matrix quality by modifying tissue age, a factor that does not vary much in mice at 16 weeks of age. In contrast, vitamins produced by the gut microbiota can influence bone tissue. In particular, vitamin K is produced by the gut microbiota and has long been associated with bone health [47,48]. Antibiotics, by modifying the gut microbiota, have long been known to be able to reduce the concentration of microbe-derived vitamin K [51]. Our findings show directly that the presence of bacterial genes required for the synthesis of vitamin K was modified by changes in the gut microbiome. Although not all of the genes required for vitamin K synthesis were depleted, reduced abundance of some genes (MenB, MenC, and MenG) can act as a rate-limiting step in menaquinone synthesis that cannot be overcome by increased abundance of other genes required for synthesis. We observed large changes in the concentration of different forms of vitamin K present in the cecum and liver. Although the greatest changes in concentration occurred in microbe-derived forms of vitamin K, little is known about the unique functional properties of the different menaquinones and additional study is required to determine the importance other than the difference in overall vitamin K concentration.
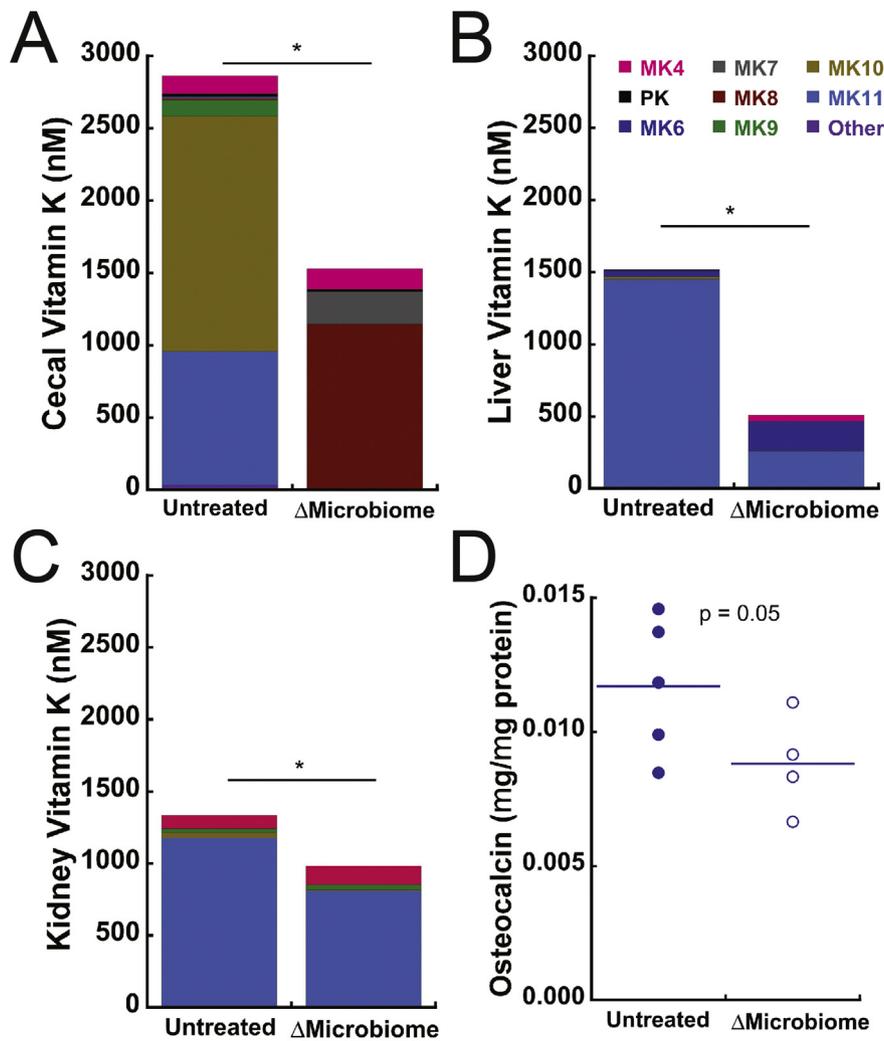
Fig. 3. Vitamin K content was altered by disruption of the gut microbiome in the (A) Cecum, (B) Liver and (C) Kidney. Each color in a column represents the average concentration of n = 6 samples (MK11 and MK13 were nondetectable, wee Supplementary Table 1). * indicates p < 0.001. (D) Matrix bound osteocalcin showed a trend indicating reduced concentration in ΔMicrobiome mice (p = 0.05).

Together with prior work, our findings provide preliminary support for a potential link between the microbiome and bone tissue quality that is mediated by microbiome-derived vitamin K. Although vitamin K may influence bone tissue quality in multiple ways, the best understood mechanism is γ carboxylation of gamma-carboxyglutamic (Gla-) containing proteins [52–54]. Vitamin K-dependent γ carboxylation is required for proper binding of Gla- containing proteins to bone tissue [52–55]. Bone contains many vitamin K-dependent proteins, however, the vitamin K-dependent protein osteocalcin is the most abundant non-collagenous protein in bone tissue and is known to influence bone tissue mechanical properties [56,57]. Interestingly, our biochemical analysis with a modest sample size suggests that ΔMicrobiome may lead to reductions in matrix-bound osteocalcin (p = 0.05). When present in bone tissue, non-collagenous proteins such as osteocalcin can regulate and direct the formation and size of collagen fibrils, as well as mineralization and crystal nucleation, leading to changes in crystallinity [58–62]. Crystallinity is descriptive of the size, perfection, and maturity of hydroxyapatite crystals and reductions in matrix crystallinity are associated with reduced bone tissue strength [63]. Bone from osteocalcin-deficient mice displays decreased crystallinity [64] and decreased bone tissue strength [65]. Similarly, we found ΔMicrobiome to lead to reduced crystallinity in this cohort of animals with impaired tissue strength (Fig. 1A). However, the literature is mixed with regard to the relationship between crystallinity (as determined here using Raman

spectroscopy) and tissue strength and have reported negative [66] as well as positive correlations between the two [63,67]. The crystallinity metric is influenced by crystal size and perfection and it is possible that the same crystallinity value can be achieved with different combinations of these two components, potentially explaining mixed findings relating crystallinity to bone strength. Nevertheless, these findings implicate vitamin K as a potential link between the microbiome and bone tissue strength, although a more thorough study that specifically tests the effect of vitamin K (rather than analyzing vitamin K to confirm metagenomic studies) is required. Hence, we cannot ignore the potential contribution of other mechanisms through which the microbiome may mediate bone. If disruption of the gut microbiome acts by modifying vitamin K, it is likely to do so at the time of bone formation (when carboxylated osteocalcin binds to bone mineral), a possibility that may make the microbiome/vitamin K status especially important during periods of rapid bone formation (growth, following anabolic treatments) as a means of ensuring that newly formed matrix has sufficient quality.

In addition to identifying differences in vitamin synthesis, the metagenomic analysis also observed significant changes in the abundance of genes associated with cell wall and capsule synthesis and carbohydrate synthesis. We attribute the differences in abundance of cell wall and capsule genes with changes in the taxonomic components of the microbiota in this cohort. Specifically, our prior taxonomic analysis
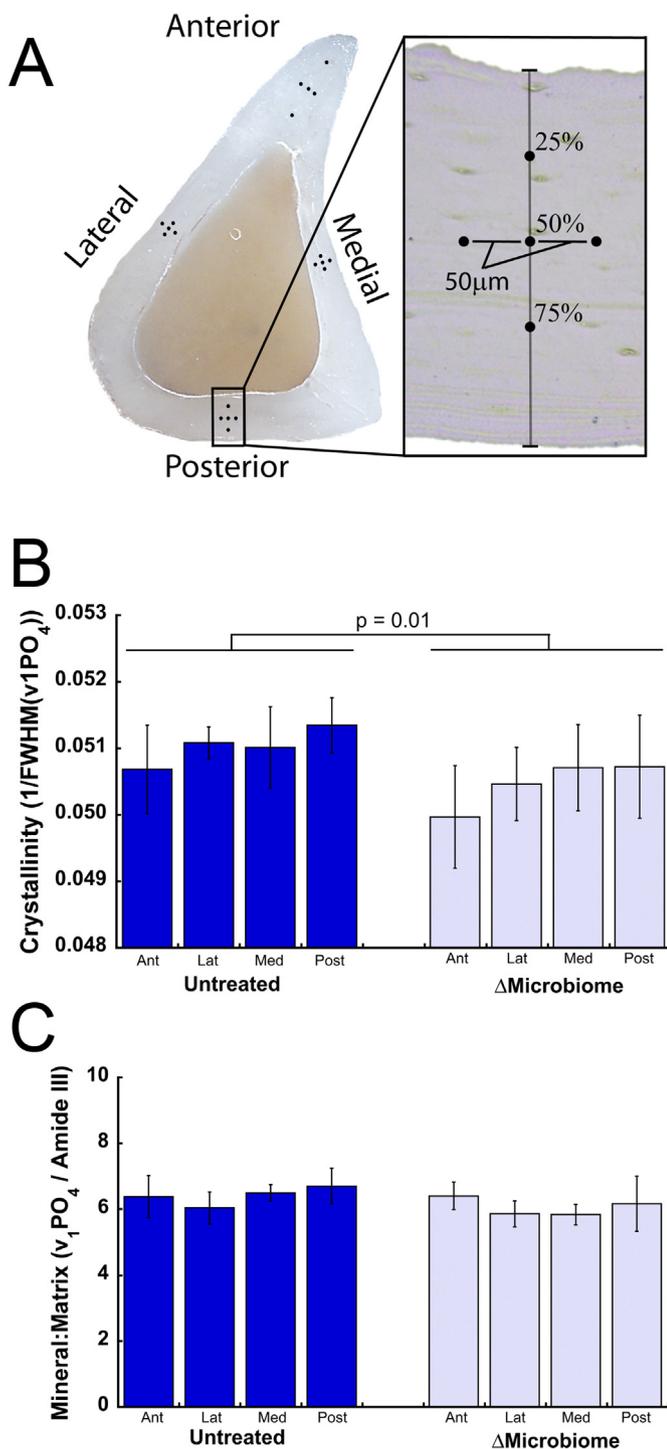
Fig. 4. (A) Five Raman point spectra were collected in each of the four anatomical quadrants of a tibial diaphysis cross section. The average of the five spectra within each quadrant was determined. ΔMicrobiome was associated with reduced (B) crystallinity and (C) no noticeable differences in mineral:matrix ratio after accounting for variation among quadrants (n = 4 specimens/group, error bars indicate SD).

associated ΔMicrobiome with increases in the abundance of organisms from the Gram negative phyla *Proteobacteria* in this cohort [8], which is consistent with the increase in the abundance of genes associated with production of Gram negative cell capsule components. In contrast, the observed changes in abundance of genes associated with carbohydrate synthesis are not as easily explained by taxonomy. These genes can influence the production of molecules such as short chain fatty acids

that have been associated with changes in bone formation and re-modeling [5], although a mechanism through which these proteins might influence bone tissue quality has not yet been proposed.

Although this cohort shows reduced tissue strength assessed in bending (Fig. 1A), we did not observe differences in nanoindentation-derived elastic modulus or hardness. Although nanoindentation derived metrics are correlated with strength in some materials, there are many materials in which there is no correlation between nanoindentation derived metrics and strength, often because the measures have different sensitivities to underlying ultrastructure of the material and the type of loading (compression v. tension). Nanoindentation-derived metrics are most sensitive to compressive properties of bone tissue while bending strength is determined primarily by tensile properties [24]. Further analysis would be required to understanding the differences in ultra-structure that generate altered tissue strength but do not alter nano-indentation-derived measures.

Several strengths in the study are worth noting. To our knowledge the current study is the first to associate changes in the microbiota metagenomic constituents with bone. Previous studies have reported changes in phylogenetic profile using 16S rRNA sequencing [3,5,8,17]. Because many different microbes have the same functional capacity, a shift in the microbial taxa may not represent differences in the functions of the microbiota. By providing the functional capacity, metagenomic analysis provides more information about potential links between the microbiome and bone. Second, to our knowledge, the current study is the first to attempt to link alterations in the gut microbiome to changes in bone tissue composition and material properties. Most previous studies have focused on how the gut microbiome can influence bone remodeling and bone density, but have not reported bone chemistry and nanoscale properties. Lastly, the vitamin K assays allowed for the differentiation between dietary and microbe-derived forms of vitamin K. Previous studies evaluating vitamin K and bone phenotype in rodents have been restricted to phylloquinone or only one menaquinone [68–70].

Despite the strengths of the current study, a few limitations must be considered when interpreting the findings. First, with regard to the metagenomic analysis, the current study was hypothesis-generating and, as molecules of interest were not known a priori, it was not possible to design the study with statistical power for all follow up biochemical assays (matrix osteocalcin in particular). Despite this limitation, the reductions in cecal and kidney vitamin K and bone tissue crystallinity in ΔMicrobiome mice and the trend toward reduced osteocalcin content were all consistent with a potential microbiome – vitamin K - matrix osteocalcin mechanism. However, the effects of vitamin K may be a result of other vitamin K-dependent molecules in bone tissue (matrix Gla protein, etc.) other ligands of vitamin K in the body (the pregnane X receptor, for example [71]) or potentially differences between carboxylated and uncarboxylated forms of osteocalcin. Second, Raman spectroscopy was performed on samples that had been fixed in formalin. Spectroscopic analysis of bone tissue is extremely sensitive to fixative. Fixation in formalin has a large effect on spectroscopic measures made using FTIR [72] and embalming and long-term storage of bone tissue can greatly influence Raman spectroscopy metrics [73]. The current study is limited to measures of mineral-to-matrix ratio and crystallinity because these two Raman spectroscopy measures are not modified by the short-term formalin fixation used in the current study [45]. Consideration of other Raman spectroscopy measures will therefore require further analysis. Additionally, although Raman spectroscopy is useful for examining chemical composition, other modifications in tissue composition may be present that are not well described by Raman spectroscopy. One limitation of the Raman spectral analysis is the use of the modestly polarization-dependent ν_1 PO_4 vibrational mode to calculate the mineral:matrix ratio, with potential variation in the outcome arising from the lamellar structure of bone. We chose the ν_1 PO_4: amide III mineral:matrix ratio because it represents a practical compromise between achieving a high signal to

noise ratio and short scan times [74] for the high density images acquired in the current study, because the v_1 PO_4 Raman band is in close proximity to other organic and inorganic bands investigated (v_1 CO_3, Amide *I*, and Amide III). Third, the biochemical analysis focused only on vitamin K in the cecum, liver, and kidney. Future studies will require a more comprehensive testing of other key potential factors such as vitamin B, circulating microbe associated molecular patterns lipopolysaccharides, and intestinal short-chain fatty acids.

In conclusion, we find that disruptions to the gut microbiome that lead to impaired bone tissue mechanical properties also lead to drastic shifts in the overall functional capacity of the gut microbiome. We observed shifts in functional capacity of the gut microbiota that were associated with changes in bone mineral crystallinity, the degree of carbonate substitution, and concentrations of microbially-derived forms of vitamin K in the body. Together our findings support the use of metagenomics for a microbiome analysis, and provide preliminary evidence for a mechanism in which production of vitamin K by the microbiota may influence downstream pathways responsible for bone tissue composition and structure.

Declaration of Competing Interest

All authors state that they have no conflicts of interest.

Acknowledgments

Authors' roles: Conceived and designed the experiments: JDG, CJH, RCB, SLB, MKS, DV, SPB, ED. Performed the experiments: JDG, SR, ZR, CHH, CJT, MKS. Analyzed data: JDG, CJH, ET. Wrote and Revised Manuscript: JDG, CJH. Critical revision and final approval of the manuscript: All authors.

We would also like to acknowledge Marysol Luna and Marjolein CH van der Meulen for their feedback in the preparation of the manuscript.

Appendix A. Supplementary data

Supplementary data to this article can be found online at https://doi.org/10.1016/j.bone.2019.06.010.

References

[1] R. Knight, C. Callewaert, C. Marotz, E.R. Hyde, J.W. Debelius, D. McDonald, M.L. Sogin, The microbiome and human biology, Annu. Rev. Genomics Hum. Genet.**18,** 18 (2017) 56–86.
[2] J.A. Gilbert, M.J. Blaser, J.G. Caporaso, J.K. Jansson, S.V. Lynch, R. Knight, Current understanding of the human microbiome, Nat. Med. 24 (4) (2018) 392–400.
[3] M. Schwarzer, K. Makki, G. Storelli, I. Machuca-Gayet, D. Srutkova, P. Hermanova, M.E. Martino, S. Balmand, T. Hudcovic, A. Heddi, J. Rieusset, H. Kozakova, H. Vidal, F. Leulier, Lactobacillus plantarum strain maintains growth of infant mice during chronic undernutrition, Science 351 (6275) (2016) 854–857.
[4] K. Sjogren, C. Engdahl, P. Henning, U.H. Lerner, V. Tremaroli, M.K. Lagerquist, F. Backhed, C. Ohlsson, The gut microbiota regulates bone mass in mice, J. Bone Miner. Res. 27 (6) (2012) 1357–1367.
[5] J. Yan, J.W. Herzog, K. Tsang, C.A. Brennan, M.A. Bower, W.S. Garrett, B.R. Sartor, A.O. Aliprantis, J.F. Charles, Gut microbiota induce IGF-1 and promote bone formation and growth, Proc. Natl. Acad. Sci. U. S. A. 113 (47) (2016) E7554–E7563.
[6] I. Cho, S. Yamanishi, L. Cox, B.A. Methe, J. Zavadil, K. Li, Z. Gao, D. Mahana,
K. Raju, I. Teitler, H. Li, A.V. Alekseyenko, M.J. Blaser, Antibiotics in early life alter the murine colonic microbiome and adiposity, Nature 488 (7413) (2012) 621–626.
[7] L.M. Cox, S. Yamanishi, J. Sohn, A.V. Alekseyenko, J.M. Leung, I. Cho, S.G. Kim, H. Li, Z. Gao, D. Mahana, J.G. Zarate Rodriguez, A.B. Rogers, N. Robine, P. Loke, M.J. Blaser, Altering the intestinal microbiota during a critical developmental window has lasting metabolic consequences, Cell 158 (4) (2014) 705–721.
[8] J.D. Guss, M.W. Horsfield, F.F. Fontenele, T.N. Sandoval, M. Luna, F. Apoorva, S.F. Lima, R.C. Bicalho, A. Singh, R.E. Ley, M.C. van der Meulen, S.R. Goldring, C.J. Hernandez, Alterations to the gut microbiome impair bone strength and tissue material properties, J. Bone Miner. Res. 32 (6) (2017) 1343–1353.
[9] Y.R. Nobel, L.M. Cox, F.F. Kirigin, N.A. Bokulich, S. Yamanishi, I. Teitler, J. Chung, J. Sohn, C.M. Barber, D.S. Goldfarb, K. Raju, S. Abubucker, Y. Zhou, V.E. Ruiz, H. Li, M. Mitreva, A.V. Alekseyenko, G.M. Weinstock, E. Sodergren, M.J. Blaser, Metabolic and metagenomic outcomes from early-life pulsed antibiotic treatment, Nat. Commun. 6 (2015) 7486.
[10] R.A. Britton, R. Irwin, D. Quach, L. Schaefer, J. Zhang, T. Lee, N. Parameswaran, L.R. McCabe, Probiotic L. reuteri treatment prevents bone loss in a menopausal ovariectomized mouse model, J. Cell. Physiol. 229 (11) (2014) 1822–1830.
[11] J.Y. Li, B. Chassaing, A.M. Tyagi, C. Vaccaro, T. Luo, J. Adams, T.M. Darby, M.N. Weitzmann, J.G. Mulle, A.T. Gewirtz, R.M. Jones, R. Pacifici, Sex steroid deficiency-associated bone loss is microbiota dependent and prevented by probiotics, J. Clin. Invest. 126 (6) (2016) 2049–2063.
[12] L.R. McCabe, N. Parameswaran, Advances in probiotic regulation of bone and mineral metabolism, Calcif. Tissue Int. 102 (4) (2018) 480–488.
[13] C. Ohlsson, D. Curiac, K. Sjogren, P. Jansson, Probiotic Treatment Using a Mix of Three Lactobacillus Strains Protects against Lumbar Spine Bone Loss in Health Early Postmenopausal Women, American Society for Bone and Mineral Research, Montreal, Canada, 2018, p. 1071.
[14] T.A. Hillier, K.L. Stone, D.C. Bauer, et al., Evaluating the value of repeat bone mineral density measurement and prediction of fractures in older women: the study of osteoporotic fractures, Arch. Intern. Med. 167 (2) (2007) 155–160.
[15] S.C. Schuit, M. van der Klift, A.E. Weel, C.E. de Laet, H. Burger, E. Seeman, A. Hofman, A.G. Uitterlinden, J.P. van Leeuwen, H.A. Pols, Fracture incidence and association with bone mineral density in elderly men and women: the Rotterdam Study, Bone 34 (1) (2004) 195–202.
[16] C.J. Hernandez, T.M. Keaveny, A biomechanical perspective on bone quality, Bone 39 (6) (2006) 1173–1181.
[17] L.V. Blanton, M.R. Charbonneau, T. Salih, M.J. Barratt, S. Venkatesh, O. Ilkaveya, S. Subramanian, M.J. Manary, I. Trehan, J.M. Jorgensen, Y.M. Fan, B. Henrissat, S.A. Leyn, D.A. Rodionov, A.L. Osterman, K.M. Maleta, C.B. Newgard, P. Ashorn, K.G. Dewey, J.I. Gordon, Gut bacteria that prevent growth impairments transmitted by microbiota from malnourished children, Science 351 (6275) (2016).
[18] T.J. Sharpton, An introduction to the analysis of shotgun metagenomic data, Front. Plant Sci. 5 (2014) 209.
[19] T. Thomas, J. Gilbert, F. Meyer, Metagenomics - a guide from sampling to data analysis, Microb Inform Exp 2 (2012) (3-3).
[20] S. Gourion-Arsiquaud, M.R. Allen, D.B. Burr, D. Vashishth, S.Y. Tang, A.L. Boskey, Bisphosphonate treatment modifies canine bone mineral and matrix properties and their heterogeneity, Bone 46 (3) (2010) 666–672.
[21] G.S. Mandair, M.D. Morris, Contributions of Raman spectroscopy to the understanding of bone strength, BoneKEy Reports 4 (2015) 620.
[22] K.-A. Kim, W. Gu, I.-A. Lee, E.-H. Joh, D.-H. Kim, High fat diet-induced gut microbiota exacerbates inflammation and obesity in mice via the TLR4 signaling pathway, PLoS One 7 (10) (2012) e47713.
[23] S. Gourion-Arsiquaud, D. Faibish, E. Myers, L. Spevak, J. Compston, A. Hodsman, E. Shane, R.R. Recker, E.R. Boskey, A.L. Boskey, Use of FTIR spectroscopic imaging to identify parameters associated with fragility fracture, J. Bone Miner. Res. 24 (9) (2009) 1565–1571.
[24] H.B. Hunt, E. Donnelly, Bone quality assessment techniques: geometric, compositional, and mechanical characterization from macroscale to nanoscale, Clinical Reviews in Bone and Mineral Metabolism 14 (3) (2016) 133–149.
[25] E.P. Paschalis, R. Mendelsohn, A.L. Boskey, Infrared assessment of bone quality: a review, Clin. Orthop. Relat. Res. 469 (8) (2011) 2170–2178.
[26] E.A. Zimmermann, R.O. Ritchie, Bone as a structural material, Adv Healthc Mater 4 (9) (2015) 1287–1304.
[27] M. Vijay-Kumar, J.D. Aitken, F.A. Carvalho, T.C. Cullender, S. Mwangi, S. Srinivasan, S.V. Sitaraman, R. Knight, R.E. Ley, A.T. Gewirtz, Metabolic syndrome and altered gut microbiota in mice lacking Toll-like receptor 5, Science 328 (5975) (2010) 228–231.
[28] D. Laukens, B.M. Brinkman, J. Raes, M. De Vos, P. Vandenabeele, Heterogeneity of the gut microbiome in mice: guidelines for optimizing experimental design, FEMS Microbiol. Rev. 40 (1) (2016) 117–132.
[29] R.R. MacGregor, A.L. Graziani, Oral administration of antibiotics: a rational alternative to the parenteral route, Clin. Infect. Dis. 24 (3) (1997) 457–467.
[30] S.F. Lima, A.G. Teixeira, C.H. Higgins, F.S. Lima, R.C. Bicalho, The upper respiratory tract microbiome and its potential role in bovine respiratory disease and otitis media, Sci. Rep. 6 (2016) 29050.
[31] F. Meyer, D. Paarmann, M. D'Souza, R. Olson, E.M. Glass, M. Kubal, T. Paczian, A. Rodriguez, R. Stevens, A. Wilke, J. Wilkening, R.A. Edwards, The metagenomics RAST server - a public resource for the automatic phylogenetic and functional analysis of metagenomes, BMC Bioinformatics 9 (2008) 386.
[32] A. Wilke, J. Bischof, W. Gerlach, E. Glass, T. Harrison, K.P. Keegan, T. Paczian, W.L. Trimble, S. Bagchi, A. Grama, S. Chaterji, F. Meyer, The MG-RAST metagenomics database and portal in 2015, Nucleic Acids Res. 44 (D1) (2016) D590–D594.
[33] R. Overbeek, T. Begley, R.M. Butler, J.V. Choudhuri, H.-Y. Chuang, M. Cohoon, V. de Crécy-Lagard, N. Diaz, T. Disz, R. Edwards, M. Fonstein, E.D. Frank, S. Gerdes,

E.M. Glass, A. Goesmann, A. Hanson, D. Iwata-Reuyl, R. Jensen, N. Jamshidi, L. Krause, M. Kubal, N. Larsen, B. Linke, A.C. McHardy, F. Meyer, H. Neuweger, G. Olsen, R. Olson, A. Osterman, V. Portnoy, G.D. Pusch, D.A. Rodionov, C. Rückert, J. Steiner, R. Stevens, I. Thiele, O. Vassieva, Y. Ye, O. Zagnitko, V. Vonstein, The subsystems approach to genome annotation and its use in the project to annotate 1000 genomes, Nucleic Acids Res. 33 (17) (2005) 5691–5702.

[34] N. Fierer, J.W. Leff, B.J. Adams, U.N. Nielsen, S.T. Bates, C.L. Lauber, S. Owens, J.A. Gilbert, D.H. Wall, J.G. Caporaso, Cross-biome metagenomic analyses of soil microbial communities and their functional attributes, Proc. Natl. Acad. Sci. U. S. A. 109 (52) (2012) 21390–21395.

[35] R.V.V. Pereira, L.M. Carroll, S. Lima, C. Foditsch, J.D. Siler, R.C. Bicalho, L.D. Warnick, Impacts of feeding preweaned calves milk containing drug residues on the functional profile of the fecal microbiota, Sci. Rep. 8 (1) (2018) 554.

[36] J.K. Goodrich, S.C. Di Rienzi, A.C. Poole, O. Koren, W.A. Walters, J.G. Caporaso, R. Knight, R.E. Ley, Conducting a microbiome study, Cell 158 (2) (2014) 250–262.

[37] B. Walther, J.P. Karl, S.L. Booth, P. Boyaval, Menaquinones, bacteria, and the food supply: the relevance of dairy and fermented food products to vitamin K requirements, Adv. Nutr. 4 (4) (2013) 463–473.

[38] T.L.A. Nguyen, S. Vieira-Silva, A. Liston, J. Raes, How informative is the mouse for human gut microbiota research? Dis. Model. Mech. 8 (1) (2015) 1–16.

[39] H.H.W. Thijssen, M.J. Drittij-Reijnders, Vitamin K distribution in rat tissues: dietary phylloquinone is a source of tissue menaquinone-4, Br. J. Nutr. 72 (3) (1994) 415–425.

[40] J.P. Karl, X. Fu, G.G. Dolnikowski, E. Saltzman, S.L. Booth, Quantification of phylloquinone and menaquinones in feces, serum, and food by high-performance liquid chromatography-mass spectrometry, J Chromatogr B Analyt Technol Biomed Life Sci 963 (2014) 128–133.

[41] T.P. Cleland, D. Vashishth, Bone protein extraction without demineralization using principles from hydroxyapatite chromatography, Anal. Biochem. 472 (2015) 62–66.

[42] E. Donnelly, S.P. Baker, A.L. Boskey, M.C. van der Meulen, Effects of surface roughness and maximum load on the mechanical properties of cancellous bone measured by nanoindentation, J. Biomed. Mater. Res. A 77 (2) (2006) 426–435.

[43] S. Gamsjaeger, A. Masic, P. Roschger, M. Kazanci, J.W.C. Dunlop, K. Klaushofer, E.P. Paschalis, P. Fratzl, Cortical bone composition and orientation as a function of animal and tissue age in mice by Raman spectroscopy, Bone 47 (2) (2010) 392–399.

[44] M. Kazanci, P. Fratzl, K. Klaushofer, E.P. Paschalis, Complementary information on in vitro conversion of amorphous (precursor) calcium phosphate to hydroxyapatite from Raman microspectroscopy and wide-angle X-ray scattering, Calcif. Tissue Int. 79 (5) (2006) 354–359.

[45] I.A.K. Fiedler, M. Casanova, T. Keplinger, B. Busse, R. Muller, Effect of short-term formaldehyde fixation on Raman spectral parameters of bone quality, J. Biomed. Opt. 23 (11) (2018) 1–6.

[46] W.C. Oliver, G.M. Pharr, An improved technique for determining hardness and elastic modulus using load and displacement sensing indentation experiments, J. Mater. Res. 7 (6) (1992) 1564–1583.

[47] R.P. Heaney, Chapter 27 - nutrition and risk for osteoporosis, in: R. Marcus, D. Feldman, J. Kelsey (Eds.), Osteoporosis, Second edition, Academic Press, San Diego, 2001, pp. 669–700.

[48] M.K. Shea, S.L. Booth, Role of vitamin K in the regulation of calcification, Int. Congr. Ser. 1297 (2007) 165–178.

[49] C.J. Hernandez, J.D. Guss, M. Luna, S.R. Goldring, Links between the microbiome and bone, J. Bone Miner. Res. 31 (9) (2016) 1638–1646.

[50] R. Pacifici, Bone remodeling and the microbiome, Cold Spring Harb Perspect Med 8 (4) (2018).

[51] J.W. Suttie, The importance of menaquinones in human nutrition, Annu. Rev. Nutr. 15 (1995) 399–417.

[52] P.V. Hauschka, J.B. Lian, P.M. Gallop, Direct identification of the calcium-binding amino acid, gamma-carboxyglutamate, in mineralized tissue, Proc. Natl. Acad. Sci. U. S. A. 72 (10) (1975) 3925–3929.

[53] P.A. Price, A.S. Otsuka, J.W. Poser, J. Kristaponis, N. Raman, Characterization of a gamma-carboxyglutamic acid-containing protein from bone, P Natl Acad Sci USA 73 (5) (1976) 1447–1451.

[54] C.M. Gundberg, J.B. Lian, S.L. Booth, Vitamin K-dependent carboxylation of osteocalcin: friend or foe? Adv. Nutr. 3 (2) (2012) 149–157.

[55] A.M. Cheung, L. Tile, Y. Lee, G. Tomlinson, G. Hawker, J. Scher, H. Hu, R. Vieth, L. Thompson, S. Jamal, R. Josse, Vitamin K supplementation in postmenopausal women with osteopenia (ECKO trial): a randomized controlled trial, PLoS Med. 5 (10) (2008) e196.

[56] S. Morgan, A.A. Poundarik, D. Vashishth, Do non-collagenous proteins affect skeletal mechanical properties? Calcif. Tissue Int. 97 (3) (2015) 281–291.

[57] A.A. Poundarik, T. Diab, G.E. Sroga, A. Ural, A.L. Boskey, C.M. Gundberg, D. Vashishth, Dilatational band formation in bone, Proc. Natl. Acad. Sci. U. S. A. 109 (47) (2012) 19178–19183.

[58] D.B. Burr, O. Akkus, Chapter 1 - Bone Morphology and Organization, Basic and Applied Bone Biology, Academic Press, San Diego, 2014, pp. 3–25.

[59] G.K. Hunter, P.V. Hauschka, A.R. Poole, L.C. Rosenberg, H.A. Goldberg, Nucleation and inhibition of hydroxyapatite formation by mineralized tissue proteins, Biochem. J. 317 (Pt 1) (1996) 59–64.

[60] M. Murshed, T. Schinke, M.D. McKee, G. Karsenty, Extracellular matrix mineralization is regulated locally; different roles of two gla-containing proteins, J Cell Bio 165 (5) (2004) 625–630.

[61] A.A. Poundarik, A. Boskey, C. Gundberg, D. Vashishth, Biomolecular regulation, composition and nanoarchitecture of bone mineral, Sci. Rep. 8 (1) (2018) 1191.

[62] S.R. Stock, The mineral–collagen interface in bone, Calcif. Tissue Int. 97 (3) (2015) 262–280.

[63] J.S. Yerramshetty, O. Akkus, The associations between mineral crystallinity and the mechanical properties of human cortical bone, Bone 42 (3) (2008) 476–482.

[64] A.L. Boskey, S. Gadaleta, C. Gundberg, S.B. Doty, P. Ducy, G. Karsenty, Fourier transform infrared microspectroscopic analysis of bones of osteocalcin-deficient mice provides insight into the function of osteocalcin, Bone 23 (3) (1998) 187–196.

[65] S. Bailey, G. Karsenty, C. Gundberg, D. Vashishth, Osteocalcin and osteopontin influence bone morphology and mechanical properties, Ann. N. Y. Acad. Sci. 1409 (1) (2017) 79–84.

[66] O. Akkus, F. Adar, M.B. Schaffler, Age-related changes in physicochemical properties of mineral crystals are related to impaired mechanical function of cortical bone, Bone 34 (3) (2004) 443–453.

[67] X. Bi, C.A. Patil, C.C. Lynch, G.M. Pharr, A. Mahadevan-Jansen, J.S. Nyman, Raman and mechanical properties correlate at whole bone- and tissue-levels in a genetic mouse model, J. Biomech. 44 (2) (2011) 297–303.

[68] M. Yamaguchi, H. Taguchi, Y.H. Gao, A. Igarashi, Y. Tsukamoto, Effect of vitamin K2 (menaquinone-7) in fermented soybean (natto) on bone loss in ovariectomized rats, J. Bone Miner. Metab. 17 (1) (1999) 23–29.

[69] G.R. Brock, G. Kim, A.R. Ingraffea, J.C. Andrews, P. Pianetta, M.C. van der Meulen, Nanoscale examination of microdamage in sheep cortical bone using synchrotron radiation transmission x-ray microscopy, PLoS One 8 (3) (2013) e57942.

[70] T. Okano, Y. Shimomura, M. Yamane, Y. Suhara, M. Kamao, M. Sugiura, K. Nakagawa, Conversion of phylloquinone (vitamin K1) into menaquinone-4 (vitamin K2) in mice: two possible routes fro menaquinone-4 accumulation in cerebra of mice, J. Biol. Chem. 283 (17) (2008) 11270–11279.

[71] T. Ichikawa, K. Horie-Inoue, K. Ikeda, B. Blumberg, S. Inoue, Steroid and xenobiotic receptor SXR mediates vitamin K2-activated transcription of extracellular matrix-related genes and collagen accumulation in osteoblastic cells, J. Biol. Chem. 281 (25) (2006) 16927–16934.

[72] S. Aparicio, S.B. Doty, N.P. Camacho, E.P. Paschalis, L. Spevak, R. Mendelsohn, A.L. Boskey, Optimal methods for processing mineralized tissues for Fourier transform infrared microspectroscopy, Calcif. Tissue Int. 70 (5) (2002) 422–429.

[73] T. Pascart, B. Cortet, C. Olejnik, J. Paccou, H. Migaud, A. Cotten, Y. Delannoy, A. During, P. Hardouin, G. Penel, G. Falgayrac, Bone samples extracted from embalmed subjects are not appropriate for the assessment of bone quality at the molecular level using Raman spectroscopy, Anal. Chem. 88 (5) (2016) 2777–2783.

[74] E.A. Taylor, A.A. Lloyd, C. Salazar-Lara, E.L. Donnelly, EXPRESS: Raman and FT-IR mineral to matrix ratios correlate with physical chemical properties of model compounds and native bone tissue, Appl. Spectrosc. 71 (10) (2017) 2404–2410 (3702817709286).